Abstract #01382 ISMRM ABSTRACT

[USGOV] Resolving and Quantifying Subvoxel Tissue Components in Multidimensional MRI for Clinical Translation

Primary: Acquisition & Reconstruction - Quantitative Imaging: relaxometry, multi-parametric, MR Fingerprinting, and synthetic MRI 〉 **Secondary:** Contrast Mechanisms - Relaxometry 〉 **Presentation:** Digital Poster, Traditional Poster, PowerPitch Oral, Oral 〉 **Keywords:** QUANTITATIVE IMAGING BIOMARKERS BRAIN TISSUE MICROSTRUCTURE BLIND SOURCE SEPARATION TISSUE COMPARTMENTS RELAXATION-DIFFUSION SPECTROSCOPY

Alexandru V Avram [1,2], **Kulam Najmudeen Magdoom**[1,2,3], **Ella Wilczynski**[1,2], **Peter J Basser**[1,2]

[1]Section on Quantitative Imaging and Tissue Sciences (SQITS), Eunice Kennedy Shriver - National Institute of Child Health and Human Development (NICHD), National Institutes of Health (NIH), Bethesda, United States of America
[2]National Institutes of Health (NIH), Bethesda, United States of America
[3]Military Traumatic Brain Injury Initiative (MTBI2), The Henry M. Jackson Foundation for the Advancement of Military Medicine, Inc., Bethesda, United States of America

Presenting Author: *Alexandru V Avram (alexandru.avram@nih.gov)*

Impact

By disentangling signals from subvoxel tissue components with distinct MR-relaxation and diffusion properties, we enable more specific and reproducible quantitative imaging biomarkers. This approach can improve clinical diagnostic sensitivity and open new avenues for investigating tissue heterogeneity and microstructural pathology.

Synopsis

Motivation: Developing sensitive MRI biomarkers for specific brain tissue components.

Goals: Resolving mixtures of microscopic tissue components with distinct T1, T2, and/or diffusion spectra in multidimensional contrast-encoded MRI (mdMRI).

Approach: Using synthetic, preclinical, and clinical datasets, we evaluate a framework that jointly estimates characteristic component spectra and their voxelwise abundances by exploiting signal correlations across many voxels.

Results: This multivoxel approach can separate tissue components even when their spectra partially overlap, enhances robustness at low SNR, and enables internal validation through bootstrapping. Compared to conventional voxelwise mdMRI reconstruction, it yields markedly improved spatial–spectral consistency, supporting more reliable and biologically specific quantitative imaging.

Introduction

Conventional MRI has limited biological specificity because it cannot resolve voxel-averaged signals into contributions from microscopic tissue components. The longitudinal and transverse relaxation times (T1, T2) and mean diffusivity (MD) are intrinsic MR-sensitive biophysical properties of water in different compartments, yet their signal contributions are superimposed within each voxel. Multidimensional contrast-encoded MRI (mdMRI) estimates voxelwise distributions (spectra) of these properties using acquisitions spanning wide ranges of joint T1-, T2-, and/or diffusion-weightings[1,2]. However, mdMRI spectral reconstruction requires solving a poorly conditioned nonlinear inverse problem. Analyzing signals from multiple voxels together can disentangle subvoxel tissue components[3]. We evaluate how leveraging inter-voxel signal-decay correlations enables identification and quantification of tissue components with well-defined mdMRI spectra in preclinical and clinical datasets.

Methods

The $N_x \times N_v$ signal-attenuation matrix $\mathbf{S}$, acquired using N_x multidimensional contrast encodings (e.g., TE/TI combinations) in N_v voxels containing mixtures of N_c subvoxel tissue components is modeled as multiplication of non-negative matrices $\mathbf{S} = \mathbf{MPF}$, where $\mathbf{M}(N_x \times N_s)$ is the known encoding matrix, $\mathbf{P}(N_s \times N_c)$ contains the unknown component spectra, and $\mathbf{F}(N_c \times N_v)$ contains the corresponding voxelwise signal fractions. We jointly estimate[3] $\mathbf{P}$ and $\mathbf{F}$ using constrained nonlinear global optimization.

We evaluated the ability to resolve mixtures of subvoxel components with partially overlapping spectra using Monte Carlo simulations across multiple SNR levels and encoding schemes. Random mixtures ($\mathbf{F}$) of three gound-truth T2-MD component specrta ($\mathbf{P}$) were generated across $N_v = 200$ voxels and signals ($\mathbf{S}$) were computed for $N_x = 12 \times 12$ joint TE-b encodings with added noise. We then jointly estimated $\mathbf{F}$ and $\mathbf{P}$ and assessed reconstruction performance.

The method was then applied to several mdMRI datasets from healthy volunteers including:

1. T1-MD data acquired with IR-prepared spherical tensor-encoded diffusion MRI[4] ($2.5 \times 2.5 \times 5mm^3$; $FOV = 220 \times 220 \times 100mm^3$; $TE/TR = 98/12000ms$; 19×16 joint T1-MD encodings, $TI = 0.05 - 5s$, $b_{STE} = 0.05 - 3.6\mu m^2/ms$), and
2. T1-T2 data acquired on an ultra-low-field 64mT portable MRI system ($2.5 \times 2.5 \times 6mm^3$; $FOV = 180 \times 220 \times 156mm^3$; 10×10 joint T1-T2 encodings, $TI = 0.05 - 1.2s$, $TR = 2s$ $TE = 5 - 374ms$).

For each dataset, we identified characteristic tissue components and evaluated their robustness as quantitative biomarkers by comparing spatial–spectral consistency to conventional voxelwise mdMRI reconstruction. Bootstrapping across voxel subsets was explored as a means for internal validation of component reproducibility.

Results and Discussion

Monte Carlo simulations using partially overlapping component spectra representative of realistic tissue environments showed that mixtures of tissue components can be disentangled by jointly analyzing signals from multiple voxels (Fig.1). The estimated component spectra and corresponding abundances closely matched ground truth values at SNR levels achievable on clinical scanners (Fig.2). As SNR decreases, signal-fraction estimates degrade before the

estimated spectra themselves. Overall, performance was less sensitive to the number of encodings (N_x), number of voxels (N_v), or number of spectral grid points (N_s), indicating robustness to typical acquisition design choices.

We repeated the *in vivo* mdMRI data analyses using different numbers of components N_c . We selected the optimal number by evaluating the spatial consistency of signal-fraction maps for components with similar spectra, though other selection methods exist[3-5]. Analysis of the ultra-low-field T1–T2 data (**Fig.3A**) revealed four distinct tissue components roughly corresponding to CSF, GM, WM, and a potential myelin-water-associated component (**Fig.3B**). Using the estimated component spectra and signal-fraction maps, we reconstructed voxelwise spectra (**Fig.3D**). This component-based reconstruction achieved substantially improved spatial–spectral consistency compared with conventional voxelwise mdMRI spectral reconstruction (**Fig.3C**). Notably, the putative myelin-water-associated component exhibited both a short-T2 peak and an intermediate-T2 feature, suggesting possible exchange processes or magnetization-transfer effects during the T1 preparation.

Analysis of the T1–MD dataset revealed three distinct tissue components roughly corresponding to CSF, GM, and WM (**Fig.4C–E**). The WM component exhibited a bimodal T1 distribution, including a small short-T1 peak potentially associated with myelin water[4,6]. We validated these findings using bootstrapping: slice voxels were randomly divided into four sets of $N_v = 765$ voxels and processed independently (**Fig.4B**). All four runs recovered highly similar spectral components (up to permutation), demonstrating methodological consistency and robust internal validation (**Fig.4A**). These results indicate that tissue-component estimation is insensitive to voxel spatial location. Spatial regularization[2], though compatible with this framework, was not used to avoid blurring in the estimated signal-fraction maps.

Conclusion

Tissue components described by non-parametric relaxation-diffusion spectra can be detected and quantified along with their relative abundances in voxel mixtures. This quantitative, data-driven framework enables internal validation and produces mdMRI spectral reconstructions with improved spatial–spectral consistency and robustness to noise for clinical applications. It could enhance quantification of components (e.g., myelin water) and reveal microstructural alterations in disease.

Acknowledgements

This work was supported by the Intramural Research Program of the Eunice Kennedy Shriver National Institute of Child Health and Human Development; NIH BRAIN Initiative 1U01EB026996-01 “Connectome 2.0: Developing the next generation human MRI scanner for bridging studies of the micro-, meso- and macro-connectome”. The contributions of the NIH author(s) are considered Works of the United States Government. The findings and conclusions presented in this paper are those of the author(s) and do not necessarily reflect the views of the NIH or the U.S. Department of Health and Human Services. This work was also partly funded by the Military Traumatic Brain Injury Initiative (MTBI2) in the Department of Defense (DoD) under award HU0001-22-2-0058. This work utilized computational resources of the NIH HPC Biowulf cluster (http://hpc.nih.gov).

References

1. Benjamini, D. & Basser, P. J. Magnetic resonance microdynamic imaging reveals distinct tissue microenvironments. NeuroImage 163, 183-196 (2017). https://doi.org/10.1016/j.neuroimage.2017.09.033

2. Kim, D., Doyle, E. K., Wisnowski, J. L., Kim, J. H. & Haldar, J. P. Diffusion-relaxation correlation spectroscopic imaging: A multidimensional approach for probing microstructure. Magnetic Resonance in Medicine 78, 2236-2249 (2017). https://doi.org/10.1002/mrm.26629

3. Slator, P. J. et al. Data-Driven multi-Contrast spectral microstructure imaging with InSpect: INtegrated SPECTral component estimation and mapping. Medical Image Analysis 71, 102045 (2021). https://doi.org/10.1016/j.media.2021.102045

4. Avram, A. V., Sarlls, J. E. & Basser, P. J. Whole-Brain Imaging of Subvoxel T1-Diffusion Correlation Spectra in Human Subjects. Frontiers in Neuroscience 15 (2021). https://doi.org/10.3389/fnins.2021.671465

5. Pas, K., Komlosh, M. E., Perl, D. P., Basser, P. J. & Benjamini, D. Retaining information from multidimensional correlation MRI using a spectral regions of interest generator. Scientific Reports 10, 1-10 (2020). https://doi.org/10.1038/s41598-020-60092-5

6. Labadie, C. et al. Myelin water mapping by spatially regularized longitudinal relaxographic imaging at high magnetic fields. Magnetic resonance in medicine 71, 375-387 (2014). https://doi.org/10.1002/mrm.24670

Figures and Tables

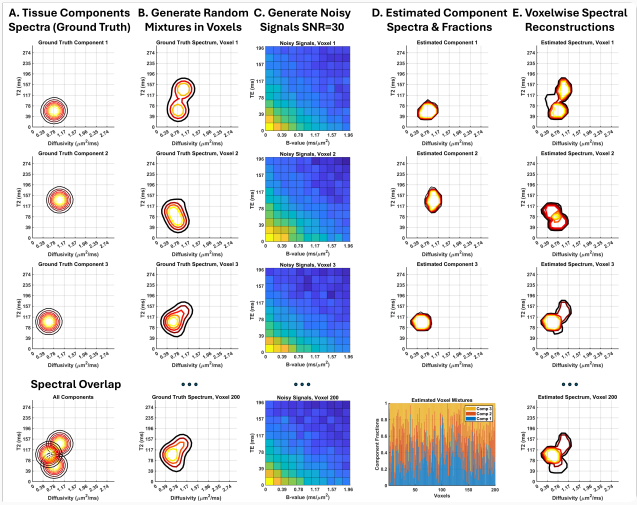

Figure 1: *Monte Carlo simulation demonstrating the ability to identify and quantify mixtures of Nc=3 tissue components with overlapping spectral peaks. By fitting noisy signals (SNR=30) from Nv=200 voxels containing arbitrary mixtures of three components with well-defined mdMRI distributions, the method accurately recovers both the ground-truth spectra and corresponding voxelwise signal fractions (Nx=12×12, Ns=24×24).*

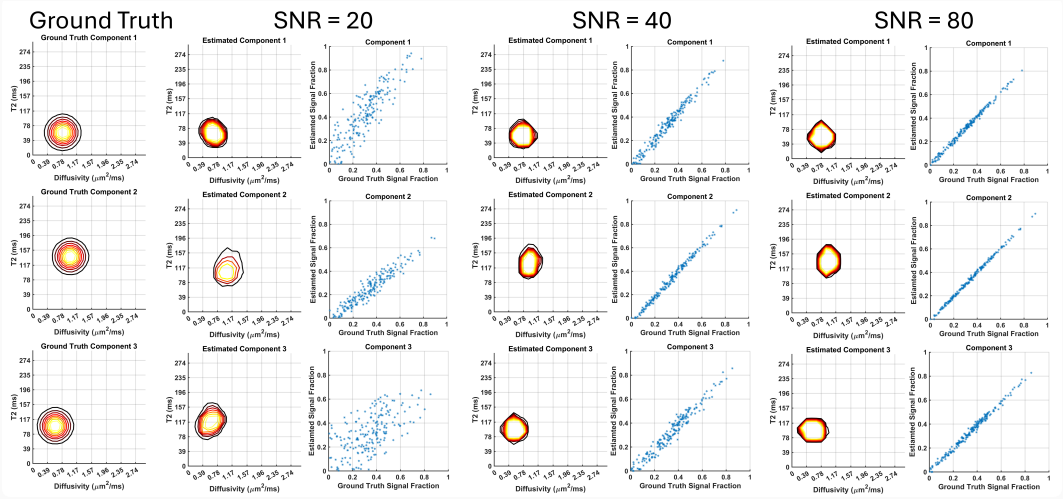

Figure 2: *Monte Carlo simulation demonstrating joint disentanglement of partially overlapping tissue-component spectra and quantification of mixture proportions in mdMRI data (Nv=200, Ns=24×24, Nx=12×12) across different SNR levels. Even at low SNR, the estimated spectra remain relatively accurate, while signal-fraction accuracy improves markedly with increasing SNR.*

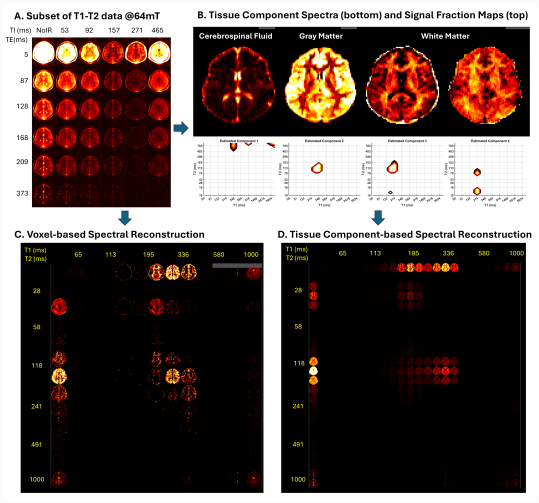

Figure 3: *Analysis of low-SNR T1–T2–encoded mdMRI data (**A**) acquired in vivo using an ultra-low-field MRI system identified four tissue components corresponding to CSF, GM, WM, and potentially myelin water (**B**). Component-based reconstruction (**D**) markedly improved spectral consistency compared with conventional voxelwise mdMRI (**C**). Nx=10×10, Nc=3, Nv=2832, Ns=12×12 (voxel-based), Ns=24×24 (component-based). In **C** and **D**, the 1D marginal distributions are shown on the left column (T2) and top row (T1).*

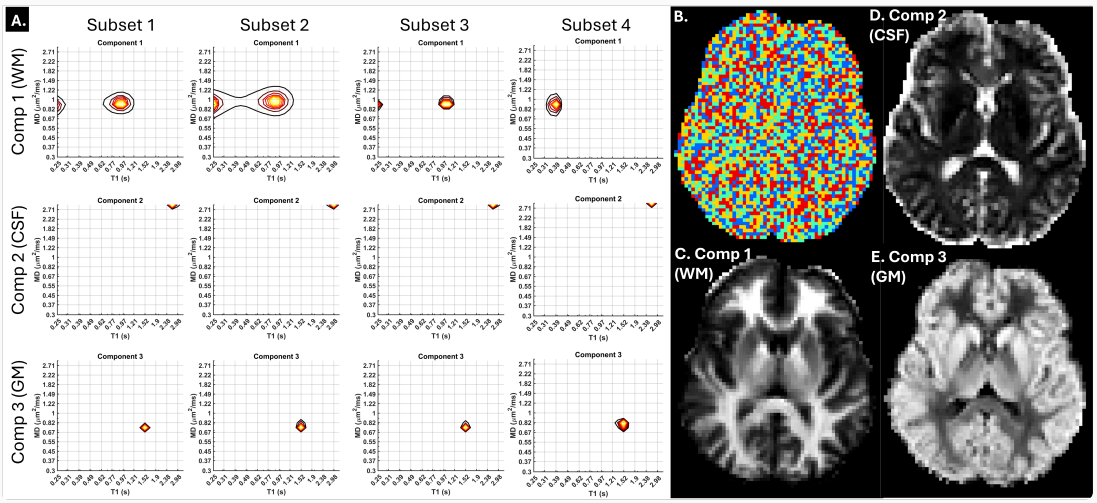

Figure 4: *Analysis of T1–MD–encoded mdMRI data acquired in a healthy volunteer on a 3T MRI system revealed three tissue components (Comp 1, 2, and 3) roughly corresponding to WM (**C**), CSF (**D**), and GM (**E**), respectively. Running the same analysis on four randomly selected voxel subsets (Nv=765 each) selected from the same slice (**B**) produced similar components (**A**), demonstrating robust internal validation. Nx=19×16, Ns=24×24.*